

Effect of hydrostatic pressure in degenerate Ge $1 - x$ Mn x Te

S. T. Lim, J. F. Bi, K. L. Teo, Feng Y. P., T. Liew, and T. C. Chong

Citation: *Applied Physics Letters* **95**, 072510 (2009); doi: 10.1063/1.3211990

View online: <http://dx.doi.org/10.1063/1.3211990>

View Table of Contents: <http://scitation.aip.org/content/aip/journal/apl/95/7?ver=pdfcov>

Published by the AIP Publishing

Articles you may be interested in

[Low-dilution limit of Zn \$_{1-x}\$ Mn \$_x\$ GeAs \$_2\$: Electrical and magnetic properties](#)

J. Appl. Phys. **114**, 093908 (2013); 10.1063/1.4820475

[Exchange interaction and Curie temperature in Ge \$_{1-x}\$ Mn \$_x\$ Te ferromagnetic semiconductors](#)

J. Appl. Phys. **110**, 023905 (2011); 10.1063/1.3610499

[Magnetic properties of IV–VI compound GeTe based diluted magnetic semiconductors](#)

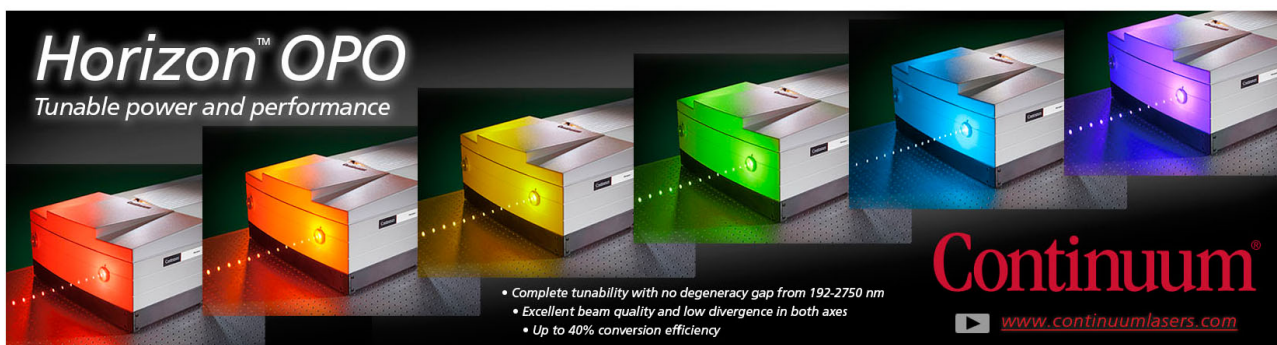
J. Appl. Phys. **93**, 7667 (2003); 10.1063/1.1556113

[Ferromagnetic properties of IV–VI diluted magnetic semiconductor Ge \$1-x\$ Mn \$x\$ Te films prepared by radio frequency sputtering](#)

J. Appl. Phys. **93**, 4034 (2003); 10.1063/1.1555697

[Carrier-enhanced ferromagnetism in Ge \$1-x\$ Mn \$x\$ Te](#)

Appl. Phys. Lett. **80**, 1013 (2002); 10.1063/1.1445477



Horizon™ OPO
Tunable power and performance

- Complete tunability with no degeneracy gap from 192-2750 nm
- Excellent beam quality and low divergence in both axes
- Up to 40% conversion efficiency

Continuum®
www.continuumlasers.com

Effect of hydrostatic pressure in degenerate $\text{Ge}_{1-x}\text{Mn}_x\text{Te}$

S. T. Lim,^{1,2} J. F. Bi,² K. L. Teo,^{2,a)} Feng Y. P.,³ T. Liew,² and T. C. Chong²

¹Graduate School for Integrative Sciences and Engineering, National University of Singapore, 28 Medical Drive, Singapore 117456, Singapore

²Department of Electrical and Computer Engineering, Information Storage Materials Laboratory, National University of Singapore, 4 Engineering Drive 3, Singapore 117576, Singapore and Data Storage Institute, 5 Engineering Drive 1, Singapore 117608, Singapore

³Department of Physics, National University of Singapore, Singapore 117542, Singapore

(Received 26 July 2009; accepted 4 August 2009; published online 21 August 2009)

We utilize the effect of hydrostatic pressure to investigate the magnetotransport properties of degenerate $p\text{-Ge}_{1-x}\text{Mn}_x\text{Te}$ ($x=0.10$) ferromagnetic semiconductor. The Curie temperature was found to increase with pressure as 0.27 K/kbar, which can be understood on the basis of the Ruderman–Kittel–Kasuya–Yosida (RKKY) interaction mechanism. For sufficiently high carrier concentration of $p_o \sim 10^{21} \text{ cm}^{-3}$, both the light holes from the L valence band and the heavy holes from the Σ valence band contribute to the RKKY interaction. Additionally, a negative magnetoresistance is observed at low temperature and is found to decrease with pressure. © 2009 American Institute of Physics. [DOI: 10.1063/1.3211990]

Recent experiments on (In,Mn)Sb under hydrostatic pressure has clearly demonstrated an increase in carrier-mediated coupling, and thus an increase in its Curie temperature T_c , as the lattice parameter is reduced by the applied pressure.¹ Tuning the exchange coupling by this process increases the magnetization, and also induces the ferromagnetic (FM) phase in an initially paramagnetic alloy. On the other hand, a decrease in T_c with applied pressure has been observed in FM $\text{Sb}_{2-x}\text{V}_x\text{Te}_3$ single crystals and the phenomenon was attributed to hole-mediated ferromagnetism within the Ruderman–Kittel–Kasuya–Yosida (RKKY) model that includes the oscillatory nature of the indirect ion–ion interaction.² Interestingly, earlier work on pressure studies in PbMnSnTe by Suski *et al.*,³ shows that the observed shift in T_c with pressure is due to the redistribution of carriers of the band structure.

In this work, we have utilized the effect of hydrostatic pressure to investigate the magnetotransport properties in degenerate $p\text{-Ge}_{1-x}\text{Mn}_x\text{Te}$. It is well known that carriers in $\text{Ge}_{1-x}\text{Mn}_x\text{Te}$ are generated by metal sublattice vacancies and the RKKY indirect exchange interaction via free carriers is responsible for the formation of the FM phase. We seek to understand the factors that influence the RKKY interaction in $\text{Ge}_{1-x}\text{Mn}_x\text{Te}$ from the magnetotransport studies under the effect of hydrostatic pressure.

A 200-nm-thick $\text{Ge}_{0.9}\text{Mn}_{0.1}\text{Te}$ thin film was grown on BaF_2 (111) substrates at $T_s=200^\circ\text{C}$ by the solid-source molecular beam epitaxy.⁴ The Mn composition was determined by x-ray photoelectron spectroscopy and the magnetic properties were investigated by a superconducting quantum interference device magnetometer. The magnetotransport measurements were carried out in an Oxford Spectromag SM400 system, which was custom designed for hydrostatic pressure measurement using an easyCell30 module up to 20 kbar and in the temperature range of 2–300 K at applied field up to 7 T. The pressure was determined using an *in situ*-calibrated manganin manometer and pentane mixture was used as the pressure transmitting medium.

Figure 1 shows the temperature dependence of the resistivity $\rho(T)$ for the $\text{Ge}_{0.9}\text{Mn}_{0.1}\text{Te}$ sample at various pressures. The magnetization $M(T)$ curve measured at ambient pressure is also depicted in the top panel. The Curie temperature $T_C=34$ K is obtained at the point of inflection of $M(T)$ curve (solid blue line) under 100 Oe field applied parallel to the plane. It can be seen that the $M(T)$ curve goes to zero at $T_C^* \sim 100$ K, which possibly originates from FM $\text{Ge}_{0.9}\text{Mn}_{0.1}\text{Te}$ clusters that give rise to magnetic short range ordering.⁵ A shallow minimum ρ_M in $\rho(T)$ at $T_R=34 \pm 10$ K is observed at ambient pressure. We have previously established that the T_R correlates directly with the T_C for different Mn compositions.⁵ The effect of an external pressure (P) on $\rho(T)$ has shifted T_R toward higher temperature (indicated by the arrows in Fig. 1) and caused a decrease in ρ .

Figure 2 shows the low temperature conductivity ($\sigma=1/\rho$) is fitted with $\sigma=\sigma_o+mT^{1/2}$ indicating that the electron–electron scattering dominates in the low temperature regime.^{6–8} In the high temperature regime, the ρ can be fitted with a power law of $\rho \propto T^{1.5}$ (red solid lines in Fig. 1) due to phonon scattering. Figure 3 displays a linear dependence of

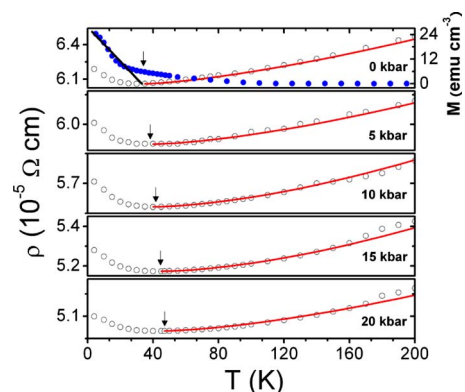


FIG. 1. (Color online) $\rho(T)$ measured at various applied pressures (open symbols) and the red solid lines are fitted to the form of $T^{1.5}$. The top panel displays the $M(T)$ curve measured at ambient pressure (solid symbols).

^{a)}Electronic mail: eleteokl@nus.edu.sg.

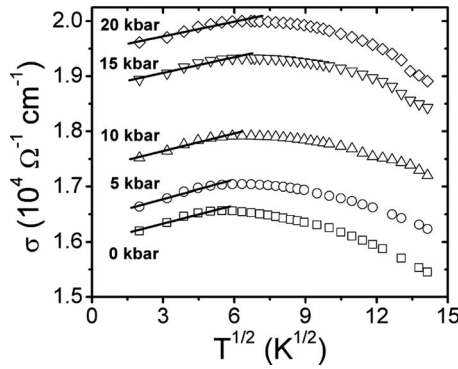


FIG. 2. Conductivities $[\sigma]$ vs $T^{1/2}$ for pressures. The solid lines are fitted with the form of $T^{0.5}$.

T_R on P with a slope of $dT_c/dP \approx dT_R/dP = 0.27$ K/kbar and a reduction in ρ_M with P . The decrease in ρ with P apparently indicates that the pressure enhances the carrier concentration (p_o). Our Hall measurement indicates that $p_o \sim 1.3 \times 10^{21}$ cm $^{-3}$ to be deep in the metallic region. We utilize the simple relation $\rho = 1/p_o q \mu$, $dp/dP = -(1/\mu q) \times (1/p_o)^2 (dp_o/dP)$ and by substituting our experimental result of $dp/dP = -5.5 \times 10^{-9}$ Ω m/kbar, we obtain $dp_o/dP = 11.4 \times 10^{24}$ m $^{-3}$ /kbar. The dT_c/dp_o can be further inferred from the relation: $dT_c/dp_o = (dT_c/dP)/(dp_o/dP)$, giving $dT_c/dp_o = 2.36 \times 10^{-26}$ K/m $^{-3}$.

In IV–VI materials such as PbTe, SnTe, and GeTe,^{9,10} the band of light holes (lh) is located at the L point of the Brillouin zone and the band of heavy holes (hh) with its top located at the Σ point below the L band. The L and Σ bands have 4 and 12 equivalent energy valleys, respectively. Within the RKKY model and the mean field theory, the T_C can be expressed as

$$T_C = \frac{2xS(S+1)}{3k_B} I_{\text{RKKY}}, \quad (1)$$

where $S=5/2$ is the Mn spin, x is the Mn composition, and I_{RKKY} is the total RKKY exchange integral, which is the sum contributions from magnetic ions interacting with free hole carriers from the valence band (VB), i.e., $I_{\text{RKKY}} = \sum_n v_n I_n$, where n is the type of valley of the band and v is the number of equivalent energy bands in that valley. We take the band structure of Ge $_{1-x}$ Mn $_x$ Te to be the same as GeTe assuming that the presence of Mn ions does not significantly alter the band structure. We first consider the case of a single VB model such that at high p_o , the Fermi level (E_F) lies inside the L band and thus only lh are involved in the interaction. Hence, the RKKY interaction can be expressed as^{11,12}

$$I_{\text{RKKY}} = v_L I_L = v_L \left[(m^*) \left(\frac{a_o^2}{2^9 \pi^3 \hbar^2} \right) \times (2k_F a_o)^4 \right] J_{pd}^2 \sum_{ij} z_{ij} F(2k_F R_{ij}) e^{-R_{ij}/\lambda}, \quad (2)$$

where $m_L^* = 1.15m_o$ is the lh effective mass, $a_o = 5.967$ Å is the lattice constant, $k_F = (3\pi^2 p_o/v_L)^{1/3}$ is the Fermi wave vector per one valley for a spherical Fermi surface with the number of equivalent energy valleys, $v_L = 4$ and $p_o = 1.3 \times 10^{21}$ cm $^{-3}$, J_{pd} is the exchange integral between holes and Mn ions, $R_{ij} = a_o \sqrt{i^2 + j^2}$ is the distance between Mn ion site i and j , z_{ij} is the number of nearest neighbors in the R_{ij} range, λ is the mean free paths of the carriers, and $F(2k_F R_{ij}) = [(\sin 2k_F R_{ij} - 2k_F R_{ij} \cos 2k_F R_{ij}) / (2k_F R_{ij})^4]$. We obtained $J_{pd} \sim 216$ meV at ambient pressure and the enhancement in J_{pd} with P , i.e., $dJ_{pd}/dP \approx 0.94$ meV/kbar. We note that Fukuma *et al.*¹³ has obtained a range of J_{pd} (0.58–0.62 eV) values for different p_o and Mn composition by considering only a single valley (i.e., $v=1$).

Next, we consider the case of the two VB model such that at sufficiently high p_o , the E_F lies inside the L band as well as the Σ band. This model was invoked to describe the physical properties of PbSnMnTe.^{11,12,14} It has been pointed out that due to the large effective mass of hh, the RKKY interaction is mostly mediated via carriers populating the Σ band. In the same vein, the increase in the p_o of Ge $_{0.9}$ Mn $_{0.1}$ Te can be further analyzed from the two VB model, which was also proposed in the pressure studies of thermopower of GeTe.¹⁵ Considering its band structure, the energy separation ΔE_v between the L and Σ bands is in the range of 0.4–0.6 eV. It has been pointed out that for $p_o \sim 10^{21}$ cm $^{-3}$, the E_F drops 0.6 eV below the L band, intersecting the Σ band in the absence of an applied P . With increasing P , the ΔE_v is diminished and the Σ band is successively promoted on the E_F level, thereby increasing p_o . The presence of more itinerant charge carriers could well enhance the RKKY interactions mechanism and hence increase the T_c . For Ge $_{0.9}$ Mn $_{0.1}$ Te with $p_o \sim 1.3 \times 10^{21}$ cm $^{-3}$, we could expect that the lh from the L band and the hh from the Σ band both contribute to the RKKY interaction, i.e., $I_{\text{RKKY}} = 4I_L + 12I_\Sigma$. In this case, $p_o = p_L + p_\Sigma$ and the parameters of the subbands can be obtained from the results of Kolomoets *et al.*,¹⁶ where the lh and hh effective masses are $m_L^* = 1.15m_o$ and $m_\Sigma^* = 5m_o$, respectively and $p_L/p_\Sigma = 3.6$. Using Eq. (1) and the respective band parameters, assuming the J_{pd} is the same for both bands, we obtained $J_{pd} \sim 78$ meV at ambient pressure and $dJ_{pd}/dP \approx 0.19$ meV/kbar. The smaller value, as compared to the case of only considering the L band, is due to the redistributions of carriers and more contribution to the RKKY interaction is attributed to the hh. Nevertheless, it is comparable to the corresponding value of 100 meV in (Pb, Sn, Mn)Te.¹¹ A $dT_c/dP \approx 0.098$ K/kbar is obtained for $p_o = 3.6 \times 10^{20}$ cm $^{-3}$ in (Pb, Sn, Mn)Te,³ which is smaller than that in Ge $_{0.9}$ Mn $_{0.1}$ Te (0.27 K/kbar). Correspondingly, a larger relative change in p_o with P is observed for Ge $_{0.9}$ Mn $_{0.1}$ Te (0.86%/kbar) than that for (Pb, Sn, Mn)Te (0.51%/kbar). In the case of (Sb, V)Te material, the increase in p_o with P has led to a suppression of ferromagnetism which was attributed to a frustrated indirect coupling led by excess carrier concentrations.² The recent report by Fukuma *et al.*¹⁷ has shown that the FM ordering of Ge $_{1-x}$ Mn $_x$ Te was

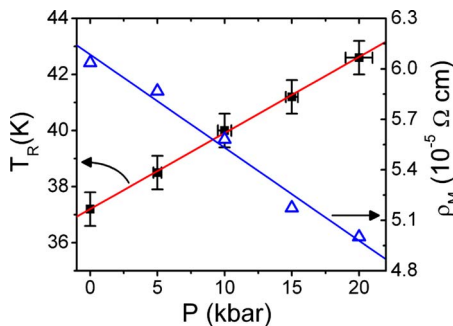


FIG. 3. (Color online) The shifts in T_R and ρ_M as functions of pressure (P).

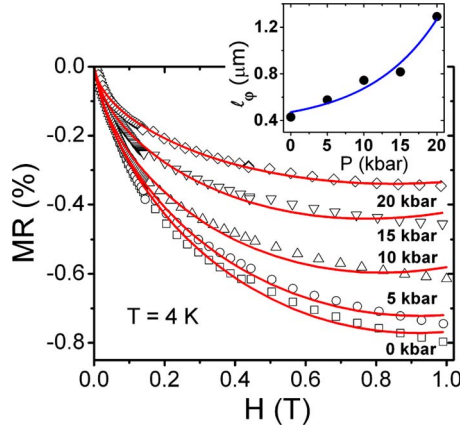


FIG. 4. (Color online) MR measured at various pressures at 4 K. The solid lines are fitted to Eq. (2). The inset shows the ℓ_ϕ vs P .

found to increase with p_o up to $3.0 \times 10^{21} \text{ cm}^{-3}$, after which it decreases with increasing p_o due to the similar effect. The frustration induced by RKKY oscillation is dominant when $p_o/n_i \gg 1$, where n_i is the impurity concentration.¹⁸ In our case, the maximum p_o at 20 kbar is $\sim 1.48 \times 10^{21} \text{ cm}^{-3}$, and thus $p_o/n_i \sim 0.78$ is less than unity. This explains the enhancement, instead of suppression, in T_C . On the other hand, there is no observation of change in p_o with P in (In, Mn)Sb while there is a slight decrease in p_o in the case of (Ga, Mn)As.¹⁹ The T_C in these materials were found to increase with P mainly due to the enhancement in J_{pd} and the band mass in according to the mean field model. It has also been found in InSb:Mn that pressure induced an increase in the exchange splitting of the acceptor hole levels and a corresponding strong reduction in p_o .²⁰

Figure 4 shows the pressure dependence of magnetoresistance (MR) at 4 K. We analyzed the negative MR at various P at 4 K by fitting it to a weak localization model²¹

$$\frac{\Delta\rho}{\rho} \approx -\frac{\Delta\sigma}{\sigma} = -(\rho) \left(\frac{e^2}{2\pi^2\hbar} \right) \left(\frac{A}{l} \right) f(x), \quad (3a)$$

$$f(x) = \sum_{N=0}^{\infty} \left\{ 2(\sqrt{N+1+x} - \sqrt{N+x}) - \frac{1}{\sqrt{N+1/2+x}} \right\}, \quad (3b)$$

$$x = \frac{\hbar}{eH} \left(\frac{1}{4} \right) \left(\frac{1}{\ell_\phi^2} \right), \quad (3c)$$

where $l = (\hbar/eH)^{1/2}$ is the magnetic length and with the constant A and phase coherence length ℓ_ϕ are used as fitting parameters. It is noteworthy that weak localization has also been observed in other materials such as $\text{Pb}_{1-x}\text{Eu}_x\text{Te}$ (Ref. 22 and (Ga,Mn)As.^{23,24} Following Prinz *et al.*,²² a prefactor a of the positive MR $\Delta\rho = aB^2$ is also included as an adjustable

parameter. The least-square fits to the MR curves are shown as solid lines for various P in Fig. 4. The inset shows the ℓ_ϕ as a function of P . As T_C increases with P , the magnetic fluctuation at low temperature is weakened, and this could lead to an increase in ℓ_ϕ with P .

In summary, we have investigated the magnetotransport properties of degenerate p - $\text{Ge}_{1-x}\text{Mn}_x\text{Te}$ with $x=0.1$. The T_C is observed to increase with pressure mainly due to the increase in carrier concentration responsible for the interactions between Mn ions. A two VB model is invoked to explain the results. The negative MR at low temperature can be attributed to the weak localization model.

This work is supported by Singapore Agency for Science, Technology and Research (A*STAR), under Grant No. 052 101 0100.

- ¹M. Csontos, G. Mihály, B. Jankó, T. Wojtowicz, X. Liu, and J. K. Furdyna, *Nature Mater.* **4**, 447 (2005).
- ²J. S. Dyck, T. J. Mitchell, A. J. Luciana, P. C. Quayle, Č. Drašar, and P. Lošťák, *Appl. Phys. Lett.* **91**, 122506 (2007).
- ³T. Suski, J. Igalson, and T. Story, *J. Magn. Magn. Mater.* **66**, 325 (1987).
- ⁴W. Q. Chen, K. L. Teo, M. B. A. Jalil, and T. Liew, *J. Appl. Phys.* **99**, 08D515 (2006).
- ⁵W. Q. Chen, S. T. Lim, C. H. Sim, J. F. Bi, K. L. Teo, T. Liew, and T. C. Chong, *J. Appl. Phys.* **104**, 063912 (2008).
- ⁶P. A. Lee and T. V. Ramakrishnan, *Rev. Mod. Phys.* **57**, 287 (1985).
- ⁷B. L. Altshuler and A. G. Aronov, in *Electron-Electron Interactions in Disordered Systems*, edited by A. L. Efros and M. Pollak (North-Holland, Amsterdam, 1985), p. 1.
- ⁸T. Dietl, *J. Phys. Soc. Jpn.* **77**, 031005 (2008).
- ⁹F. Herman, R. L. Kortum, I. B. Ortenburger, and J. P. Van Dyke, *J. Phys. (Paris)* **29**, C4 (1968).
- ¹⁰J. E. Lewis, *Phys. Status Solidi B* **59**, 367 (1973).
- ¹¹T. Story, G. Karczewski, L. Świerkowski, and R. R. Gałazka, *Phys. Rev. B* **42**, 10477 (1990).
- ¹²T. Story, P. J. T. Eggenkamp, C. H. W. Swiiste, H. J. M. Swagten, W. J. M. de Jonge, and L. F. Lemmens, *Phys. Rev. B* **45**, 1660 (1992).
- ¹³Y. Fukuma, H. Asada, N. Nishimura, and T. Koyanagi, *J. Appl. Phys.* **93**, 4034 (2003).
- ¹⁴H. J. M. Swagten, W. J. M. deJonge, R. R. Gałazka, P. Warmenbol, and J. T. Devreese, *Phys. Rev. B* **37**, 9907 (1988).
- ¹⁵L. G. Khvostantsev and V. A. Sidorov, *Phys. Status Solidi B* **116**, 83 (1983).
- ¹⁶N. V. Kolomoets, E. Ya. Lev, and L. M. Sysoeva, *Sov. Phys. Solid State* **6**, 551 (1964).
- ¹⁷Y. Fukuma, H. Asada, S. Miyawaki, T. Koyanagi, S. Senba, K. Goto, and H. Sato, *Appl. Phys. Lett.* **93**, 252502 (2008).
- ¹⁸S. Das Sarma, E. H. Hwang, and D. J. Priour, Jr., *Phys. Rev. B* **70**, 161203(R) (2004).
- ¹⁹M. Csontos, G. Mihály, B. Janko, T. Wojtowicz, W. L. Lim, X. Liu, and J. K. Furdyna, *Phys. Status Solidi C* **1**, 3571 (2004).
- ²⁰J. Teubert, S. A. Obukhov, P. J. Klar, and W. Heimbrodt, *Phys. Rev. Lett.* **102**, 046404 (2009).
- ²¹A. Kawabata, *Solid State Commun.* **34**, 431 (1980).
- ²²A. Prinz, G. Brunthaler, Y. Ueta, G. Springholz, G. Bauer, G. Grabecki, and T. Dietl, *Phys. Rev. B* **59**, 12983 (1999).
- ²³F. Matsukura, M. Sawicki, T. Dietl, D. Chiba, and H. Ohno, *Physica E (Amsterdam)* **21**, 1032 (2004).
- ²⁴L. P. Rokhinson, Y. Lyanda-Geller, Z. Ge, S. Shen, X. Liu, M. Dobrowolska, and J. K. Furdyna, *Phys. Rev. B* **76**, 161201(R) (2007).